ISSN: 03875547
Volume 45, Issue 08, October, 2022

Antitumor effects of novel biosynthesized shelled copper nanostructures in comparison to copper oxide nanoparticles on tumor bearing mice by an epigenetic modulating mechanism

Nehad Naem Hamed Shosha[1*], Ola Mohamed Samy Ahmad Sadek[1], Sameh Hamed Ismail[2], Radwa Wahid Mohamed[1]

Department of Biochemistry and Nutrition; Women's college for Arts Science and Education, Ain Shams University, Cairo, Egypt[1]
Faculty of Nanotechnology for Postgraduate Studies, Cairo University, Sheikh Zayed Campus, 6th October City, Giza, 12588, Egypt[2]

Corresponding Author: 1*

Keywords:
Copper nanoparticles, miRNA-34a, P53, antitumor, CA15-3.

ABSTRACT

The use of plant extracts in the biosynthesis of nanoparticles displayed superiority over other biological agents and had and promising strategies for anticancer treatment. This study explored the antitumor effect of biosynthesized copper nanoparticles shelled with turmeric, sumac and vitamin B12 as core-shell or core-double-shell nanostructures at genetic and epigenetic levels and evaluate these nanomaterials side effect on hemopoietic, liver and kidney status in comparison to CuO nanoparticles on tumor bearing mice. All nanomaterials synthesis and characterization were done to confirm the successful synthesis. To conduct this study female mice were injected with Ehrlich Ascites carcinoma cells and then treated with either one of the nanostructures or CuO nanoparticles. Antitumor effect of nanomaterials was evaluated by measurement of tumor volume and serum CA15-3 level. miRNA-34a, and P53 RNA expression were also measured. Side effect of these nanomaterials' treatment were assessed by screening the complete blood picture and measurement of liver and kidney functions. All nanomaterials significantly diminished tumor growth and CA15-3 level. Although, it seems that CuO nanoparticles showed the most significant reduction in tumor volume, the other nanostructures have higher impact on miRNA-34a and p53 RNA expression moreover, they attenuated the hematological, liver and kidney biomarkers more than CuO NPs did. Using turmeric nanostructures has more powerful effect than Sumac nanostructures otherwise adding vitamin B12 as second shell improve the nanostructures efficiency. The biosynthesized nanostructures induced much deeper effect on epigenetic and genetic levels and attenuated the side effects of nanomaterial treatments than chemically synthesized CuO NPs.

1. INTRODUCTION

Cancer treatment strategies have been seriously restricted by their side effects which urges us to develop new technologies for more effective and much safer anticancer therapies. Novel nanomedicine, based on different kinds of functional nanomaterials, have been proved to act as effective and promising strategies for anticancer treatment [1]. The use of plant extracts in the preparation of metallic nanoparticles (NPs) as a convenient substitute for physical and chemical methods has been proposed and displayed superiority over other biological agents. Nanoparticles synthesized using plant extracts exhibit various pharmaceutical and therapeutic effects [2].

Plants have been employed in biosynthesizing metal/metal oxide NPs due to their capping and reducing properties. This biosynthesis approach allows the production of the desired NPs in different sizes and shapes by manipulating parameters during the synthesis process. The most commonly used metals and oxides are gold (Au), silver (Ag), and copper (Cu). Among these, Cu is a relatively low-cost metal that is more cost-effective than Au and Ag [3].

Copper oxide nanoparticles (CuO NPs) have been widely studied owing to their physical, biochemical, and pharmacological features. Cu-based products have exhibited toxicity to many cancer cells [4], [5]. However, previous studies demonstrated that the exposure of mice to copper nanoparticles (CuNPs) or CuO NPs resulted in severe kidney, and liver impairment [6], [7]. Other purpose of plant derived nanoparticle products have the potential to be hepatoprotective and therefore can be used modulate the nanoparticles hepato-nephrotoxicity [8].

The challenge is to identify promising natural compounds aid the therapeutic effect of CuNPs and provide more advanced genetic and epigenetic antitumor mechanisms. Turmeric (Tur), *Curcuma longa* is very well-known medicinal plant not only in the Asian hemisphere but also known across the globe for its therapeutic and medicinal benefits. The active moiety of *Curcuma longa* is curcumin and has gained importance in various treatments of various disorders such as bacterial infection, cancer, obesity, diabetics, and wound healing applications [9]. Previous studies proved the ability of curcumin to modulate several signalling pathways and biomolecules in cancer with significant epigenetic mechanisms [10]. Safety and cost-effectiveness are additional inevitable advantages of curcumin [11]. Otherwise, Curcumin nanoparticles efficiently attenuate the hepatotoxicity and nephrotoxicity caused by cancer chemotherapy [12].

Sumac (Sum), *Rhus coriaria L***.** is a traditional herb; its leaves and fruits show therapeutic effects on a wide range of diseases. Sumac is gifted with several biological properties including antioxidant, antiinflammatory [13], hypoglycemic, and hypolipidemic activities [14]. This could refer to Sum composition and promising functional compounds such as flavonoids phenolic acids and tannins [15]. The bioactive compounds in Sum extract that potentially induce anticancer effects were previously identified **[**16]. Sumac extract was used for Au [17], and Ag [2] nanoparticles biosynthesis to display superior antioxidant and further biological active component for metallic NPs.

Vitamin B12 (vit B12) is an essential nutrient for cell proliferation. Vitamin B12 is an attractive entity for tumor diagnostic and possible therapeutic applications [18]. Vitamin B12- conjugated nano-micelles were exhibited cancer targeting abilities and enhanced cellular drug uptake on gastric cancer cells [19].

Nanostructure-mediated drug delivery, a key technology for the realization of nanomedicine, has the potential to improve drug bioavailability, and ameliorate side effects of drug molecules. Along with these wide applications, this study concerns about the possible antitumor effect of CuNPs biosynthesized with Tur, Sum,

and vit B12 as core-double-shell or core-shell nanostructures on tumor bearing mice. It is also crucial to evaluate the safety and impact of these biosynthesized nanostructures on hepato-renal toxicity induced either by tumor itself or as a side effect of CuNPs treatment.

2. MATERIAL AND METHODS

2.1 Materials

Murine Ehrlich ascites carcinoma (EAC) cells were obtained from the oncology unit, The National cancer institute (NCI), Cairo University, Egypt. Turmeric (Tur), and Sumac (Sum) were purchased from Ministry of Agriculture, Giza, Egypt. Copper oxide nanoparticles (CuO NPs), copper sulfate, vit B12 and vitamin C were purchased from Sigma Aldrich Company, USA.

2.2 Synthesis of core-shell and core-double-shell copper nanostructures

Copper nanoparticles (CuNPs) were biosynthesized by the precipitation method using copper sulfate and vitamin C (as reducing agent) assisted by the sonochemical method [20]. All Copper core-shell and core-double-shell nanostructures were synthesized by a sonochemical method using biosynthesized CuNPs dispersed in deionized distilled water as described previously [7]. Copper with vit B12 or with Tur core-shell nanostructure (Cu+B12 NS), (TurCu NS) were synthesized by adding CuNPs to either Methylcobalamin film or Tur solution then both mixtures were subjected to ultrasonic irradiation, precipitated, washed, and dried. Similarly, copper with sumac core-shell nanostructure (SumCu NS) was synthesized after preparation of Sum water extract by boiling 10g Sum in 150 ml deionized water for 2hours, then freeze-drying the extract. (TurCu+ B12 NS) or (SumCu+ B12 NS) core-double -shell nanostructures were synthesized by adding either TurCu NS or SumCu NS to Methylcobalamin film and subjected to ultrasonic irradiation as mentioned before.

2.3 Characterization of CuO nanoparticles, core-shell, and core-double-shell copper nanostructures:

Characterization of CuO NPs and the other biosynthesized nanostructures were done to using Transmission Electronic Microscope (TEM) [Jeol, JEM-2100 high-resolution, Japan], and Atomic force microscope (AFM) [5200LS, Agilent, USA] to confirm nano-scale morphology. Crystal properties of all nanomaterials were examined by X-ray powder diffraction (XRD) [40Kv and 40 mA with 2 theta measure range from 10 to 90º using XRD instrument Rigaku smart lab. Jaban].

2.4 Animal

Eighty healthy female mice weighing 20-30 g were used. The animals were were supplied from the oncology unit – National Cancer Institute (NCI), Cairo University, Egypt. All experiments were conducted following the guidelines for the care and use of experimental animals. mice were maintained on a standard commercial pellets diet and tap water *ad libitum* (24) and kept in stainless cages with a constantly controlled environment; temperature 25°C ± 5°C, air humidity 55% ± 10%, and 12/12 hrs light/dark were held.

2.5 Experimental design

Mice were divided into eight groups 10 mice each. Ten mice were served as normal control group. The rest of mice (70 mice) were inoculated with a single intramuscular (IM) injection of 2.5 x106 EAC/ml in the right thigh to form a solid tumor as described previously [20] and kept till tumor appeared then tumor bearing mice were subdivided into 7 groups 10 mice served as tumor bearing group and each subgroup treated with intratumor injection by chemically synthesized CuO NPs or one of the biosynthesized nanostructures 3 times per week for 2 weeks as showed in (figure. 1).

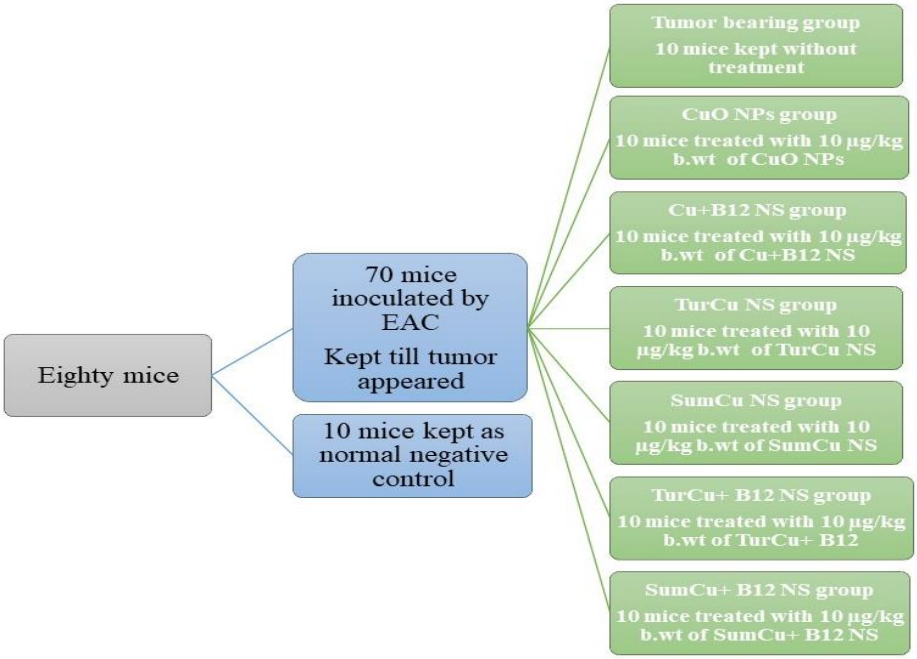

Figure (1): Diagram of the experimental design.

2.6 Sampling

At the end of experimental period, all mice were scarified after 12 hours fasting with water *ad libitum* and blood was collected and separated into two parts. One part of the blood samples was collected as whole blood in EDTA-containing tubes. Another part of blood samples was allowed to stand for 15 min and then centrifugated at 3000 rpm for 15 min. Serum was kept in plastic vials at -20^{o}C until used for biochemical analyses. Tumor tissues were stored frozen at -80^{o}C for biochemical and gene expression analyses.

2.7 Biochemical analyses

2.7.1 Measurement of complete blood count (CBC):

The numerical counts of the cellular fractions of the blood red blood cells (RBCs) and white blood cells (WBCs), as well as hemoglobin concentration were measured, also hematological indices including mean corpuscular hemoglobin (MCH), mean corpuscular hemoglobin concentration (MCHC), hematocrit (HCT) and mean corpuscular volume (MCV), were determined using an automatic hematological assay analyzer, Advia 60 Hematology system [Bayer Diagnostics Europe Ltd, Ireland].

2.7.2 Assessment of liver functions:

Liver functions were assessed by measurement of serum aspartate and alanine aminotransferases activities (AST, ALT) using kinetic AST/SGOT and ALT/SGPT kits, cat no: EZ013LQ, and cat no: EZ017LQ, respectively, purchased from Reactivos GPL, Barcelona, Spain.

2.7.3 Assessment of kidney functions:

Serum urea and creatinine were measured by end point colorimetric urea and creatinine kits, cat no: SU040, and cat no: SU015, respectively, purchased from Reactivos GPL, Barcelona, Spain.

2.7.4 Measurement of serum tumor marker Carbohydrate Antigen 15-3 (CA-15.3):

Mice CA-15.3 tumor marker was measured by Enzyme linked immunosorbent assay (ELISA) technique using CA-15.3 ELIZA kit, cat no: MBS2502096, My BioSource, San Diego, USA.

2.7.5 MiRNA-34a and P53 RNA gene expression in tumor tissues:

Tissue homogenization was prepared using Tissue Ruptor II kit, Qiagen, Hilden, Germany. Tissue samples were homogenized in the presence of lysis buffer in 15–90 seconds, using a rotor–stator homogenizer depending on the toughness and size of the sample. Then the mixture was centrifugated for 20 minutes at 4000rpm. The cell supernatant was collected for RNA extraction. Total mRNA was extracted using miReasy Mini Kit, Qiagen, Hilden, Germany, according to the manufacturer's protocol. Finally, cDNA was synthesized by reverse transcription reaction using mi Script RT Kit, Qiagen, Hilden, Germany.

M22iR-34a expression analysis: The quantification of, miR-34a gene expression levels were amplified from miRNA extract using a miScript primer assay; [Hs_miR-34a] Primer Assay. The miRNAs genes were amplified by miScript Syber green Master mix, Qiagen, Hilden, Germany. The SNORA73 Primer Assay was used as housekeeper gene. The PCR reaction mix was prepared by adding as follow, 5µL of 2x miScript Syber green Master mix, 10x miScript Universal (1µL) 10x miScript Hs_miR-34a Primer Assay(1µL), template cDNA(1µL), and RNase-free water were thawed at room temperature (15-25ºC). Then, the final volume reached 10 µl per well reaction volume by the addition of 2 µL of RNase-free water. The reaction mix was mixed thoroughly but gently, and dispensed appropriate volumes into the Rotor-Disc wells and the disc was sealed with Rotor-Disc Heat-Sealing Film. All samples were analysed using the 5 plex Rotor-Gene PCR Analyzer, Qiagen, Germany.

Consequently, the real-time cycler initial was programmed as: activation step for 15 minutes at 95ºC for HotStarTaq DNA Polymerase activation. Three-step cycling: denaturation for 15 seconds at 94ºC, annealing for 30 seconds at 55ºC, extension for 30 seconds at 70ºC, for 40 cycles. Moreover, the expression levels were normalized to SNORA73 levels as a reference gene. The relative expression level (fold change) for miR-34a was normalized to an internal control (SNORA73) and relative to calibrator (negative control sample) were calculated using the equation 2-ΔΔCt test control.

P53 expression analysis : The P53 gene expression level was amplified from mRNA using QuantiTect primer assay [Hs_TP53, QuantiTect Primer Assay, cat no: 249900], Qiagen, Germany and QuantiTect SYBR Green PCR Kit cat no: 204141, Qiagen, Germany, and Hs_ACTB_1_SG QuantiTect Primer Assay (β-actin) cat no: 249900, as housekeeper gene. All samples were analyzed using the 5 plex Rotor Gene PCR Analyzer, Qiagen, Germany. The PCR reaction mix was prepared for a final volume 18 µl per well reaction volume as following: 10 µl of 2x QuantiTect SYBR Green PCR Master Mix, 2 µl 10x t Universal Primer, 2 µl 10x Quantitect Primer Assay and 4 µl RNase-free water. The reaction mix was mixed thoroughly but gently, and dispensed appropriate volumes into the Rotor-Disc wells then 2 µl template cDNA was added, to reach 20 µl as final volume. Carefully, tightly the disc was sealed with Rotor-Disc Heat-Sealing Film. The real-time cycler initial was programmed, the calibration and calculation were done as described before in miRNA concerning the β-actin levels as a reference gene.

2.8 Statistical analysis

Results were analysed using the Statistical Package for Social Science (SPSS) program, version 16. The data were expressed as mean ± standard deviation (S.D) of the mean. The statistical difference was preformed between groups using one way analysis of variance (ANOVA). The mean difference was significant at $P < 0.05$ level [21].

3. RESULTS

3.1 Characterization of CuO NPs and other Cu core-shell and core-double-shell nanostructures

XRD pattern as shown in (figure 2) illustrated the presence of cubic crystal Cu nanoparticles with amorphous area refer to Tur, Sum and Vit B12 according to database number COD 4105681 of Burcker eva software database while CuO nanoparticles (fig. 2-S6) database number was COD9015924.

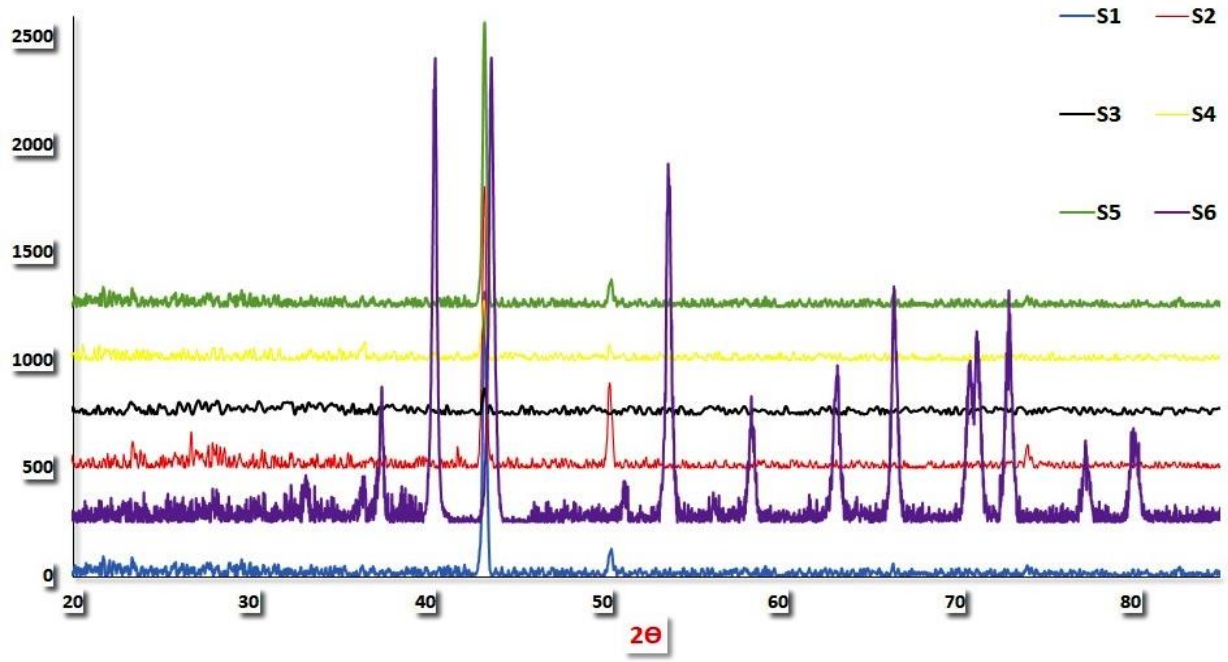

Figure (2): XRD pattern of S1) TurCu NS, S2) TurCu+B12 NS, S3) SumCu+B12 NS, S4) SumCu NS, S5) Cu+B12 NS, and S6) CuO NPs.

The different TEM and AFM images illustrated the formation of core-shell and core-double shell nanostructures. However, TEM images as shown in (figure 3A) illustrated the homogenous in shape and size of core-shell nanostructure with sub-spherical cores of teeth edges and smooth spherical shells. TEM images illustrate the size of samples about 90 nm. CuO nanoparticles TEM image illustrated the spherical shape with 19 nm size. AFM images also as shown in (figure 3B) showed the sub-spherical shape of nanomaterials with homogenous in shape and size.

ISSN: 03875547
Volume 45, Issue 08, October, 2022

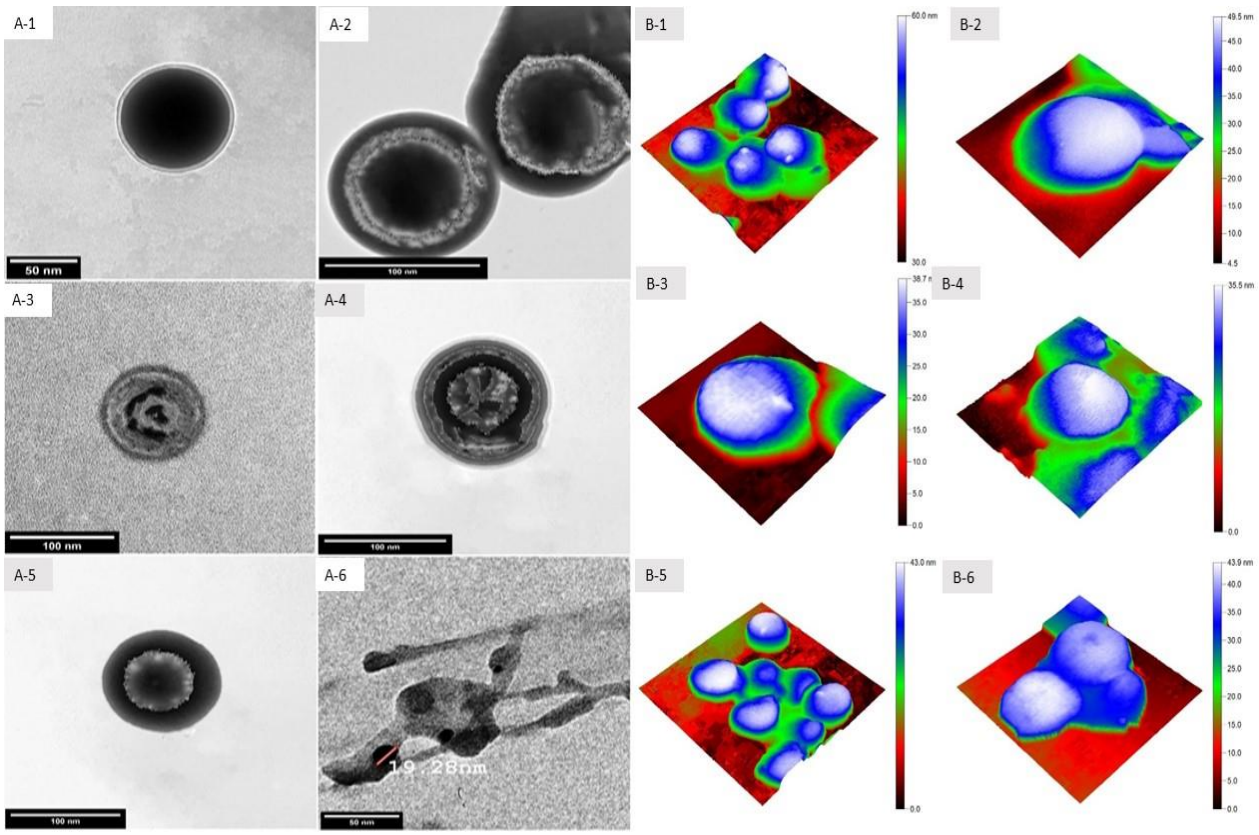

Figure (3): A) TEM image and B) AMF image of 1) Cu+B12 NS, 2) TurCu NS, 3) TurCu+B12 NS, 4) SumCu NS, 5) SumCu+B12 NS, and 6) CuO NPs.

3.2 Effect of copper nanostructures on complete blood picture of tumor bearing mice

Results illustrated in (Table 1) indicated that tumor bearing group exhibited anemia indicated by a significant decrease in RBCs count, Hb, HCT, MCH. MCHC% with a significant increase in MCV level compared to normal control group. Also, tumor bearing group significantly exhibited thrombocytosis with a significant reduction in white cell count compared to control group. Generally, treatment with any of nanostructures or CuO NPs significantly alleviated tumor bearing induced anemia. Comparing to CuO NPs group, treatment with other nanostructures caused non-significant elevation ($P < 0.05$) in MCHC%. Anemic parameter non-significantly elevated by treatment of Cu+B12 NS compared to CuO NPs. Meanwhile, injection of TurCu+B12 NS caused the most significant modulation in anemic status compared to CuO NPs.

Table (1): Complete blood picture for tumor-bearing groups injected with different form Copper nanostructures.

	RBCs (10^6)	Hb	HCT	MCV	MCH	MCHC %	Platelet (10^3)	WBCs (10^6)
Control	5.99± 0.60	16± 0.69	45.52± 3.90	74.81± 3.58	28.5 ± 1.08	35.86± 0.84	204± 9.63***	15.7± 1.53
Tumor-bearing	3.39± 0.69***	7.5± 1.58	29± 4.32	103.± 4.73	22.48± 0.92	26.09± 0.93	304 ± 40.7	7.5 ± 1.08
CuO NPs	3.4± 0.43**	11± 0.77	34± 2.58	95.78± 3.40	26.35± 1.22	32.33± 1.10	175± 21.26*	8.23± 0.60**
Cu+B12 NS	3.9± 0.52**,***	11.7± 1.45***	34.42± 3.78***	94.05± 4.19***	26.7± 1.09***	32.51± 1.03***	214± 25.43*	12.03± 1.04

TurCu NS	3.7± 0.63**,***	10.3± 0.42***	39.50± 2.99	86.22± 2.31	27.43± 0.95*,***	31.79± 0.91***	254 ± 11.41	10.09± 0.87
TurCu+B12 NS	4.53± 0.66	12.52± 1.07	33± 2.96	88.39± 2.39	28.02± 0.72*	32.12± 1.07***	247 ± 52.23	13.4± 1.11
SumCu NS	3.13± 0.26**,***	10.5± 0.06***	31± 5.06**,***	70.73± 4.5	28.8± 2.02*	33.13± 0.86***	200± 8.16*,***	9.14± 0.91
SumCu+B12 NS	4.35± 0.48	10.91± 1.15***	32± 2.66**,***	87.77± 4.14	28.61± 2.68*	32.71± 1.27***	176± 33.16*,***	13.26± 1.29

Values are represented as mean ±SD., (n=10), (P< 0.05). (*), (**), and (***) indicated non-significant differences from control, tumor-bearing, and CuO NPs groups respectively.

The platelets count was significantly decreased after treatment with any of the nanostructures. CuO NPs, Cu+B12 NS, SumCu NS, and SumCu+B12 NS caused a nonsignificant decrease ($P < 0.05$) in platelet count compared to normal control group. SumCu NS platelet count was the nearest value to control group. Regarding WBCs tumor-bearing group had a significant reduction in white blood cell count compared to normal control group indicating the presence of leukopenia. Treatment with CuO NPs caused non-significant ($P <0.05$) elevation in WBCs compared to tumor bearing group. Meanwhile, treatment with the other copper nanostructures caused significant WBCs elevation compared to both CuO NPs and tumor bearing groups.

3.3 Effect of copper nanostructures on liver and kidney functions of tumor bearing mice

Data obtained in (Table 2) Revealed that AST and ALT activities were significantly ($P < 0.05$) elevated in tumor-bearing group compared to normal control group. Injection of CuO NPs or any of the other Cu nanostructures caused significant reduction ($P < 0.05$) in both AST and ALT activities compared to tumor bearing group. TurCu NS caused non-significant reduction ($P < 0.05$) in ALT activity compared to normal control. Additionally, vitamin B12 containing nanostructures as core-double-shell caused the least elevation in AST activity compared to normal control group. Meanwhile, Cu shelled with vitamin B12 as core-shell nanostructure caused non-significant increase ($P< 0.05$) in ALT activity compared to CuO group.

Results illustrated kidney functions in (Table 2) as urea and creatinine levels indicated that tumor bearing group had significant increase ($P < 0.05$) in both kidney function parameters compared to normal control group. CuO NPs treated mice were significantly reduced ($P < 0.05$) urea level and non-significantly reduced creatinine level compared to tumor bearing group. Although, other nanostructures treatment except SumCu NS were non-significantly increased creatinine level compared to normal control group.

Table (2): Liver and kidney functions of tumor-bearing mice injected with copper nanostructures

	AST	ALT	Urea	Creatinine
Control	10.57 ± 0.55	13.5 ± 1.08	15.4 ± 0.67	0.61 ± 0.06
Tumor-bearing	19.12 ± 1.08	36.63± 1.97	26.83 ± 0.44	1.3 ± 0.39
CuO NPs	13.42 ± 0.32	27.61 ± 0.92	18.57 ± 0.72	1.14± 0.24**
Cu+B12 NS	11.94 ± 0.63	28.11 ± 0.87***	16.7 ± 0.9	0.61 ± 0.06*
TurCu NS	12.6 ± 0.67	12.09 ± 1.35*	16.67 ± 0.96	0.77 ± 0.08*
TurCu+B12 NS	10.5 ± 0.57*	15.7 ± 0.82	17.12 ± 0.52	0.74 ± 0.14*
SumCu NS	11.6 ± 0.89	18.26 ± 3.55	16.8 ± 0.87	0.91 ± 0.07
SumCu+B12 NS	11.07 ± 0.71*	21.03 ± 1.97	17.8 ± 0.85***	0.67 ± 0.16*

Values are represented as mean ±SD., (n=10), (P< 0.05). (*), (**), and (***) indicated non-significant differences from control, tumor-bearing, and CuO NPs groups respectively.

ISSN: 03875547
Volume 45, Issue 08, October, 2022

3.4 Effect of copper nanostructures on tumor growth and tumor marker (CA15-3) of tumor bearing mice

Results in (Figure 4) showed that serum tumor marker CA15-3 elevated significantly ($P < 0.05$) by 687.9% in tumor bearing group compared to normal control group. Treatment by any of nanomaterials caused significant reduction in CA15-3 level compared to tumor bearing group. Sum nanostructures caused significant increase ($P < 0.05$) in CA15-3 level by 237.3% and 210.8% for SumCu NS and SumCu+ B12 NS respectively compared to control group. Cu+B12 NS and TurCu NS treatment caused non-significant ($P < 0.05$) increase in CA15-3 by 30.1% and 5.66 % respectively, that almost reach the level of normal control group. Otherwise, CuO NPs and TurCu+B12 NS groups caused further reduction in CA15-3 level compared to normal control.

Results of CA15-3 was confirmed by the results of tumor volume and morphology illustrated in (figure 5a) which indicated that tumor volume was significantly decreased ($P < 0.05$) after treatment with any nanostructures compared to tumor bearing group. Treatment with CuO NPs caused the highest significant decrease in tumor volume by - 96.4% meanwhile, treatment with SumCu NS caused the least significant reduction in tumor volume by -72.8% compared to tumor bearing group. Adding Vit B12 as double-shell improve the effect of nanostructures compared to that without Vit B12 on the tumor growth indicated by the significant reduction in tumor volume and confirmed by the morphological changes as showed in (figure 5b).

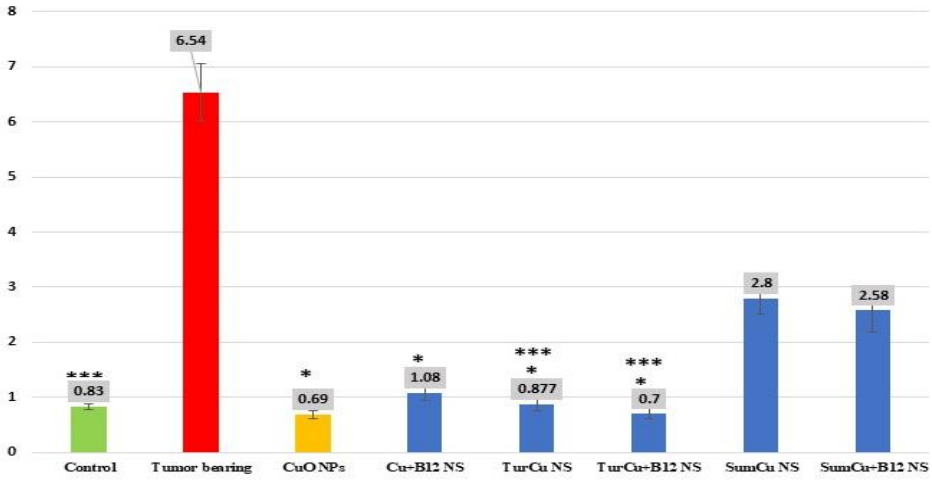

Figure 4: Serum CA15-3 level of tumor-bearing mice injected with copper nanostructures. Values are represented as mean ±SD., (n=10), (P< 0.05). (*), (**), and (***) indicated non-significant differences from control, tumor-bearing, and CuO NPs groups respectively.

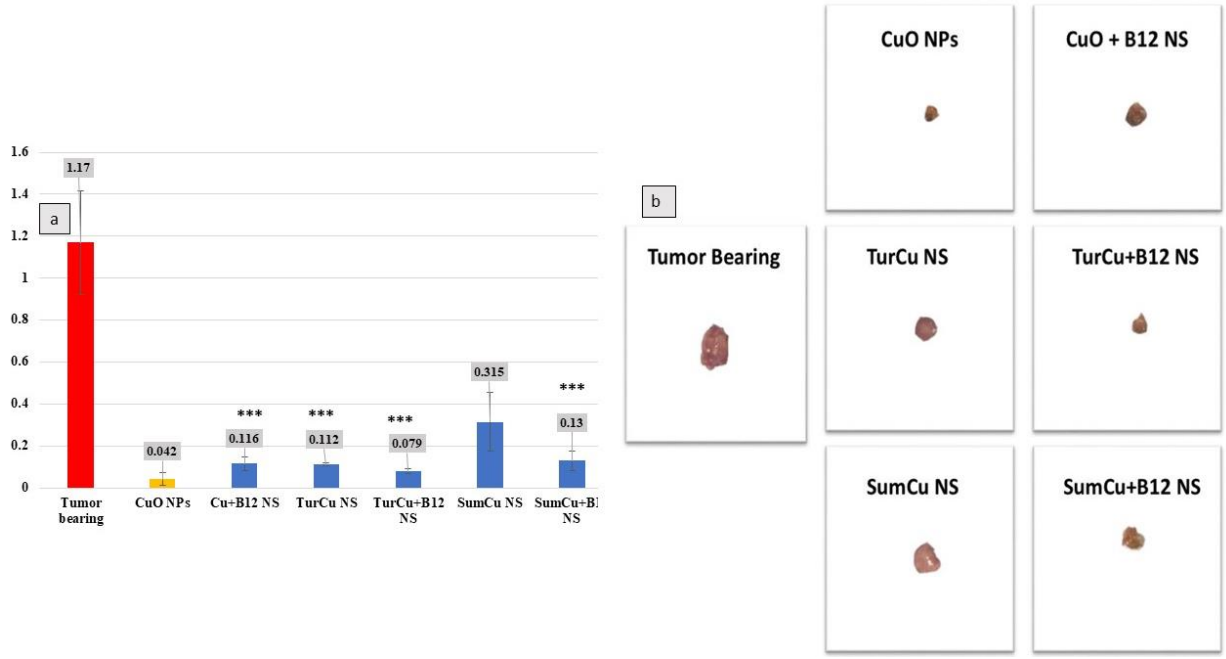

Figure 5: Tumor volume (a) and morphology (b) of tumor-bearing mice injected with copper nanostructures. Values are represented as mean ±SD., (n=10), (P< 0.05). (**), and (***) indicated non-significant differences from tumor-bearing, and CuO NPs groups respectively.

3.5 Effect of copper nanostructures on expression of miRNA-34a and P53 genes of tumor bearing mice

MicroRNAs (miRNAs) represent a new class of prognostic epigenetic marker as well as new therapeutic targets in cancer therapy. The tumor suppressor miR-34 family, represent a downregulated component of tumor suppressor p53 network. Results of the present work Fig. 6a showed that all treated groups have significant elevation ($P < 0.05$) in miRNA-34a expression compared to untreated tumor bearing group. TurCu+B12 NS caused the highest significant elevation ($P < 0.05$) in miRNa-34a expression although CuO NPs caused the least significant increase ($P < 0.05$) in miRNA-34a expression compared to tumor bearing group. That reflected on the P53 expression as the results showed in Fig. 6b indicated that CuO NPs caused significant reduction ($P < 0.05$) in P53 expression compared to tumor bearing group. On the other hand, treatment with the biosynthesized nanostructures caused significant elevation in P53 gene expression compared to tumor bearing group. Adding vitamin B12 as core-double shell nanostructure significantly improve the expression of miRNA-34a and consequently the P53 expression as compared to CuO NPs or the other nanostructures.

ISSN: 03875547
Volume 45, Issue 08, October, 2022

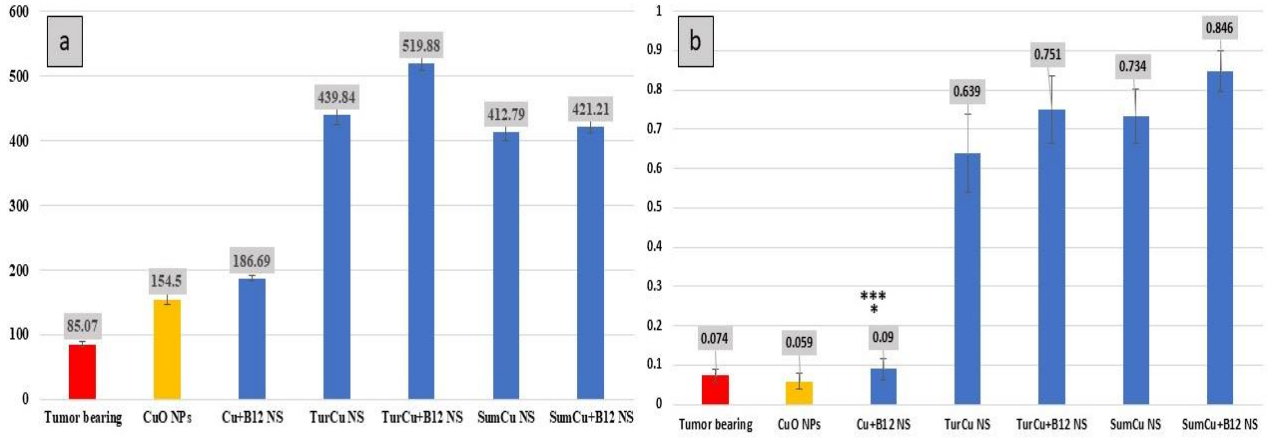

Figure (6): Expression of miRNA (a) and P53 (b) genes of tumor-bearing mice injected with copper nanostructures. Values are represented as mean ±SD., (n=10), (P< 0.05). (**), and (***) indicated non-significant differences from tumor-bearing, and CuO NPs groups respectively.

4. Discussion

This study conducted to assess the antitumor effect of novel CuNP biosynthesized with Tur, Sum, and VitB12 as core-shell or core-double-shell nanostructures in comparison to CuO NPs on tumor bearing mice at genetic and epigenetic levels and the possible consequence side effects on hematological parameter, and hepato-nephrotoxicity. The current results confirmed that all nanostructures were synthesized successfully in nanoscale.

Many blood-based biomarkers have been exploited as an ideal biomarker allowing detection of cancer at its earliest stages [22]. Tumor induced abnormal granule-monocyte differentiation of hematopoietic stem cells, affecting the distribution and function of haemocytes in tumor bearing mice. Tumor bearing mice peripheral blood had decreased the RBC, HGB, HCT, and neutrophils percentage [23]. Moreover, Platelets have been shown to possess an important biological role at several stages of malignant disease, such as angiogenesis, cell proliferation, cell invasiveness, and metastasis [24]. In addition, there are indications that inhibition of platelet function has an inhibitory effect on tumor growth and that this increases overall survival of patients [25]. It has been suggested that targeting platelets may result in inhibition of cancer progression. Indeed, reduction of platelet count in tumor bearing mice reduced tumor angiogenesis, tumor growth, and metastasis [24] that was observed in the current results after treatment with any of the nanomaterials. Furthermore, cancers are involved with dysregulated inflammation because multiple types of leukocytes exist in the tumor microenvironment. Leukocytes circulate in bloodstream and are recruited to inflammation sites or a tumor microenvironment, so they could be employed as a carrier to deliver nanotherapeutics to inflammatory or tumorous sites. Nanoparticles can either attach to or be internalized in cells, and then they move together without changes in leukocyte functions [26].

Results from the current study revealed that tumor induced anemia and leukopenia. On the other hand, treatment with CuO and other Cu nanostructures modulate the changes in hemopoietic parameters induced by tumor growth. CuO NPs caused the least effect although using Tur, Sum or Vit B12 as a copper NPs shell restore the CBC more than CuO NPs did. Using vitamin B12 as a double shell for TurCu and SumCu nanostructures caused the most advanced effect on all hemopoietic picture.

Nano-copper caused strong hepatic toxicity by inducing oxidative stress and inflammation [27]. It has been proven that CuNPs are extremely reactive and simply interact with other particles, leading to a wide range of biological activities. The liver is considered the key target tissue of drug toxicity. Hence, assessing the function of this organ is a very important method to determine drug toxicity [28]. The present work showed that CuO NPs modulate the liver and kidney functions of tumor bearing mice that may related to its amelioration of tumor growth status that affect on liver and renal toxicity, as indicated from the results that CuO NPs cause the highest elimination in tumor volume that also related to the reduction in CA15-3 tumor marker.

Meanwhile the core-shell nanostructures were more effective in modulating the hepato-renal functions disrupted by induction of tumor. Using vit B12 as double-shell for Tur or Sum Cu-nanostructures aid the strength of these nanostructures in controlling the hepato-renal toxicity induced by tumor growth. As previously confirmed that, CuNPs biosynthesized from aqueous extract of *C. spinosa* fruit have no toxic effects on the liver functions and hematological parameters of mice [29]. Moreover, curcumin – the main turmeric active component- effectively protect against hepatotoxicity induced by ZnO NPs in rats. Furthermore, the significant increase in serum activity of ALT, AST, and ALP activities induced by ZnO NPs was attenuated by Curcumin treatment [30]. Also, dietary Curcumin induced hepatoprotective role with the AgNPs used in EAC induced tumor [8].

Hepatotoxicity of chemotherapeutic agents have been well documented. However, the introduction of new classes of therapies such as small molecule inhibitors and immunotherapies have introduced new hepatotoxicity challenges and management strategies [31]. This work showed that Tur and Sum shelling of Cu-nanostructures have double positive effect observed as attenuated the growth of tumor tissues and reduce the hepatorenal toxicity that always combined the tumor therapy. This effect related to the active component of Tur or Sum that help to reduce the Cu NPs toxicity and aid their antitumor effect. Otherwise, Vit B12 showed adverse increase in the antitumor activity of their nanostructures even if, it had no change or may worsen the hepto-renal status. Vit B12 has anticancer effects, but one main issue is that cells do not uptake the needed amount of vitamin to exert an antitumor effect when it is administered as such [32]. VitB12-loaded solid lipid nanoparticles can improve the vitamin uptake by cells and the anticancer properties of the vitamin and be specific for cancer cells [33].

MicroRNAs is a group of small endogenous noncoding RNAs has recently emerged. They can act as either oncogenes or oncosuppressors depending on their target genes. miRNAs are gaining significant interest due to their translational application as therapeutic agent and epigenetic mechanism targets in the management of disease [34]. Among miRNAs, miRNA-34a has been connected with both tumor repression and autophagy regulation, and its expression is frequently lost in many cancers. Therefore, enforced expression of miRNA-34a in cancer cells may represent a valid strategy to reduce cancer growth [35].

The current study confirmed that treatment of tumor bearing mice with CuO NPs had limited effect on miRNA-34a gene expression. Meanwhile, adding Tur or Sum to Cu core-Shell nanostructure directly elevated the miRNA-34a expression that may be related to active component that add advanced effect to the biosynthesized Cu nanostructure.

Curcumin that naturally derived from the rhizome of Tur and is known to have antioxidant and anticarcinogenic properties. When curcumin was added to the human breast carcinoma (MDA MB 231) cell line in which miR 34a was knocked down, there was a decrease in anti miR 34a in curcumin treated cells in comparison to the untreated cells [36]. Furthermore, it was found that curcumin significantly upregulated the

expression of miR-34a, in prostate cancer cell lines. Expression of miR-34a altered cell cycle-related genes expression and significantly played an important role in the antiproliferation effect of curcumin in prostate cancer [37] and endothelial cancer [38]. It seems that Sum had a similar effect on miRNA-34a that nearly approach that of Tur. Finding from this study showed that adding Vit B12 to Cu nanostructures as core-shell or core-double-shell improve the nanostructures ability to increase the expression of miRNA-34a. Previously it was observed that exposure to vitamin B12 perinatal and postnatal supplementation overexpressed miR-34a level [39].

MiR-34a is involves in certain epithelial-mesenchymal transition (EMT)-associated signal pathways to repress tumorigenesis, cancer progression, and metastasis. Due to the particularity of miR-34 family in tumor-associated EMT, the significance of miR-34a is being increasingly recognized [40]. The tumor-suppressor miR-34 family, a downstream component of the p53 network, inhibited in various solid malignancies [41]. P53, the most commonly mutated gene in human cancer, is essential for maintaining the stability of the human genome [42], [43]. Its loss is a key event in the development of various tumors [44]. P53 expression plays an important role in protecting cells from malignant transformation by inducing cell cycle arrest or apoptosis [45]. The current finding showed that CuO NPs had no effect on P53 expression even the other biosynthesized nanostructures highly increase the expression of P53 RNA their advanced impact may be matched with their epigenetic effect on miRNA-34a.

5. Conclusion

The application of metal nanoparticles in cancer treatment widely spread, although limitation of their usage come from their possible side effects. Here, using the novel copper nanostructures biosynthesized with Tur, Sum, and Vit B12 had antitumor effect. They also had deeper effect on epigenetic and genetic levels indicated by upregulation of miRNA-34a expression and the related P53 RNA. Although CuO NPs were effective in reducing tumor growth, the biosynthesized nanostructures had the ability to attenuate the side effects induced by nanomaterial treatment as indicated by the reduction in the elevated liver and kidney function, and modulating effect on anemia, leukopemia, thrombocytopenia combined with tumor induction.

6. References

[1] Huang H., Wang J., Zhang J., Cai J., Pi J., & Xu J. Inspirations of cobalt oxide nanoparticle based anticancer therapeutics. Pharmaceutics. 2021;13: 1-26. https://doi.org/10.3390/pharmaceutics13101599.

[2] Ghorbani P., Namvar F., Homayouni-Tabrizi M., Soltani M., Karimi E. & Yaghmaei P. Apoptotic efficacy and antiproliferative potential of silver nanoparticles synthesized from aqueous extract of sumac (Rhus coriaria L.). IET Nanobiotechnol. 2018; 12(5): 600-603. https://www.researchgate.net/publication/322776426

[1] Letchumanan D., Sok S. P. M., Ibrahim S., Nagoor N.H., & Arshad N. M. Plant-Based Biosynthesis of Copper/Copper Oxide Nanoparticles: An Update on Their Applications in Biomedicine, Mechanisms, and Toxicity. Biomolecules. 2021; 11(4):1-27. doi: 10.3390/biom11040564.

[2] Tabrez S., Khan A.U., Mirza A.A., Suhail M., Jabir N.R., Torki A., Zughaibi T.A., & Alam M. Biosynthesis of copper oxide nanoparticles and its therapeutic efficacy against colon cancer. Nanotechnology Reviews. 2022; 11(1): 1322– 1331.

[3] Zughaibi T.A., Mirza A.A., Suhail M., Jabir N.R., Zaidi S.K., Wasi S., Zawawi A., & Tabrez S. Evaluation of anticancer potential of biogenic copper oxide nanoparticles (CuO NPs) against breast cancer.

J. Nanomaterials. 2022: 1-7. https://doi.org/10.1155/2022/5326355.

[4] Yang J., Hu S., Rao M., Hu L., Lei H., Wu Y., Wang Y., Ke D., Xia W., & Zhu C. Copper nanoparticle-induced ovarian injury, follicular atresia, apoptosis, and gene expression alterations in female rats. Inter. J. Nanomedicine. 2017;12: 5959–5971.

[5] Shosha N.N.H., Mohamed R.W., Ismail S.H., & Sadek, O.M.S.A. Amelioration of potential hazard of copper nanoparticles by bio-synthetic methods using novel Turmeric (Curcuma longa), Sumac (Rhus coriaria L.), and Vitamin B12 shelled nanostructures. Teikyo medical journal. 2022; 45(4): 6445-6460.

[6] Abou El-Fotoh M.F., Abou-Hadeed A.H., & Kotb, E.K.G. Toxicological effects on silver nanoparticles as anticarcinogenic agent and its treatment with curcumin. Zagazig Veterinary Journal. 2017: 45 (S1): 296-304. DOI: 10.21608/zvjz.2017.29250.

[7] Chopra H., Dey P.S., Das D., Bhattacharya T., Shah M., Mubin S., Maishu S.P., Akter R., Rahman H., Karthika C., Murad W., Qusty N., Alshammari Q.S., Batiha G.E., Altalbawy F.M.A., Albooq M.I.M. & Alamri B.M. Curcumin Nanoparticles as Promising Therapeutic Agents for Drug Targets. Molecules. 2021; 26:1-25. https://doi.org/10.3390/molecules26164998.

[8] Hassan F., Rehman M.S., Khan M.S., Ali M.A., Javed A., Nawaz A., & Yang C. Curcumin as an alternative epigenetic modulator: mechanism of action and potential effects. Front. Genet. 2019; 10(514):1-16. doi: 10.3389/fgene.2019.00514.

[9] Talib W.H., Al-hadid S.A., Ali M.B., & Abdel-Razik A.N., Role of curcumin in regulating p53 in breast cancer: an overview of the mechanism of action. Breast Cancer - Targets and Therapy. 2018; 10:207-217. doi: 10.2147/BCTT.S167812.

[10] El-Gizawy M.M., Hosny E.N., Mourad H.M., et al. Curcumin nanoparticles ameliorate hepatotoxicity and nephrotoxicity induced by cisplatin in rats. Naunyn. Schmiedebergs. Arch. Pharmacol. 2020; 393:1941–1953. https://doi.org/10.1007/s00210-020-01888-0.

[11] Morshedloo M.R., Fereydouni S., Ahmadi H., Hassanpouraghdam M.B., Aghaee A., Mehrabani L.V., & Magg F. Natural diversity in fatty acids profiles and antioxidant properties of sumac fruits (Rhus coriaria L.): Selection of preferable populations for food industries. Food Chem. 2022; 374: 1-10. https://doi.org/10.1016/j.foodchem.2021.131757.

[12] Kazemi S., Shidfar F., Ehsani S., Adibi P., Janani L., & Eslami O. The effects of sumac (Rhus coriaria L.) powder supplementation in patients with non-alcoholic fatty liver disease: A randomized controlled trial. Complement. Therap. Clin. Pract. 2020; 41: 1-6. https://doi.org/10.1016/j.ctcp.2020.101259.

[13] Farag M.A., Fayek N. M., & Abou Reidah I. Volatile profiling in Rhus coriaria fruit(sumac) from three different geographical origins and upon roasting as analyzedvia solid-phase microextraction. PeerJ., 2018; 6: 1-16. http://dx.doi.org/10.7717/peerj.5121.

[14] Abdallah S., Abu-Reidah I., Mousa A., & Abdel-Latif T. Rhus coriaria (sumac) extract reduces migration capacity of uterus cervix cancer cells. Barazillian Journal pharmacology., 2019; 29: 591–596. https://doi.org/10.1016/j.bjp.2019.06.004.

[15] Shabestarian H., Homayouni-Tabrizi M., Soltani M., Namvard F., Azizif S., Mohamad R., & Shabestarian, H. Green Synthesis of Gold Nanoparticles Using Sumac Aqueous Extract and Their Antioxidant Activity. Materials Research. 2017; 20(1):264-270. DOI: http://dx.doi.org/10.1590/1980-5373-MR-2015-0694.

[16] Chen Z., Liang Y., Feng X., Liang Y., Shen G., Huang H., Chen Z., Yu J., Liu H., Lin T., Chen H., Wu D., Li G., Zhao B., Guo W., & Hu, Y. Vitamin-B12-conjugated PLGA-PEG nanoparticles incorporating miR-532-3p induce mitochondrial damage by targeting apoptosis repressor with caspase recruitment domain (ARC) on CD320-overexpressed gastric cancer. Mater. Sci. Eng. C. Mater. Biol. Appl. 2021; 120:1-12. doi: 10.1016/j.msec.2020.111722..

[17] Guo W., Deng Z., Chen L., Chen Z., Yu J., Liu H., Li T., Lin T., Chen H., Zhao M., Zhang L., Li G., & Hu Y. Vitamin B12-conjugated sericin micelles for targeting CD320-overexpressed gastric cancer and reversing drug resistance, Nanomedicine (Lond)., 2019; 14 (3): 353–370, https://doi.org/10.2217/nnm-2018-0321.

[18] Ismail S., Mohamed G., Amer A., & Amer M. Comparative Killing Activity of Different Nanoparticles and Nanocomposites Based on Dermanyssusgallinae. Nano Biomed. Eng., 2020; 12(4): 338-350. DOI: 10.5101/nbe.v12i4.p338-350.

[19] Abdl-Dayem S.A.E., Foda F., Helal M., Zaazaa A., & Fahmy A. The role of catechin against doxorubicin--induced cardiotoxicity in Ehrlich Ascites Carcinoma Cells (EAC) bearing mice. J. Am. Sci., 2010; 6(4): 146-152.

[20] Levesque R. SPSS programming and data management: A Guide for SPSS and SAS user. 4rd Edition, SPSS Inc, Chicago, IL. 2007.

[21] Guo W., Chen Y., Shi R., He K., Wang J., Shao J., Wan J., & Gao J. 20(S)-Protopanaxdiol suppresses the abnormal granule-monocyte differentiation of hematopoietic stem cells in 4T1 breast cancer-bearing mouse. Evid. Based. Complement. Alternat. Med., 2020:1-11. https://doi.org/10.1155/2020/8747023.

[22] Sabrkhany S., Kuijpers M.J.E., Egbrink M.G.A., & Griffioen A.W. Platelets as messengers of early-stage cancer. Cancer and Metastasis Rev., 2021; 40(2):563–573. https://doi.org/10.1007/s10555-021-09956-4.

[23] Lucotti S., Cerutti C., Soyer M., Gil-Bernabé A.M., Gomes A.L., Allen P.D., Smart S., Markelc B., Watson K., Armstrong P.C., Mitchell J.A., Warner T.D., Ridley A.J., & Muschel R.J. Aspirin blocks formation of metastatic intravascular niches by inhibiting platelet-derived COX-1/thromboxane A2. J. Clin. Invest., 2019; 129(5):1845–1862. doi: 10.1172/JCI121985.

[24] Dong X., Chu D. & Wang Z. Leukocyte-mediated delivery of nanotherapeutics in inflammatory and tumor sites. Theranostics., 2017; 7(3): 751- 763. doi: 10.7150/thno.18069.

[25] Tang H., Xu M., Luo J., Zhao L.; Ye G., Shi F., Lv C., Chen H., Wang Y., & Li Y. Liver toxicity assessments in rats following sub-chronic oral exposure to copper nanoparticles. Environ. Sci. Eur., 2019; 31(30): 1-14. https://doi.org/10.1186/s12302-019-0214-0.

[26] Mahmoudvand H., Fallahi S., Mahmoudvand H., Shakibaie M., Harandi M.F., & Dezaki E.S. Efficacy of Myrtus communis L. to inactivate the hydatid cyst protoscoleces, J Invest Surg., 2016; 29:137-143. doi: 10.3109/08941939.2015.1088601. Epub 2015 Dec 18.

[27] Khatami M. Ebrahimi K. Galehdar N. Moradi M.N., & Moayyedkazemi A. Green synthesis and characterization of copper nanoparticles and their effects on liver function and hematological parameters in mice. Turk. J. Pharm. Sci., 2020; 17(4):412-416. DOI: 10.4274/tjps.galenos.2019.28000.

[28] Khorsandi L., Mansouri E., Orazizadeh M. & Jozi Z. Curcumin attenuates hepatotoxicity induced by zinc oxide nanoparticles in rats. Balkan. Med. J., 2016; 33:252-257. DOI: 10.5152/balkanmedj.2016.150017.

[29] Mudd T.W., & Guddati A. K. Management of hepatotoxicity of chemotherapy and targeted agents. Am. J. Cancer Res., 2021; 11(7):3461-3474. www.ajcr.us /ISSN:2156-6976/ajcr0131115.

[30] Fidaleo M., Tacconi S., Sbarigia C., Passeri D., Rossi M., Tata A.M., & Dini L. Current nanocarrier strategies improve vitamin B12 pharmacokinetics, ameliorate Patients' Lives, and Reduce Costs. Nanomaterials (Basal)., 2021; 11(743):1-19. https://doi.org/10.3390/nano11030743.

[31] Genç L., Kutlu H.M., & Güney G. Vitamin B12-loaded solid lipid nanoparticles as a drug carrier in cancer therapy. Pharm. Dev. Technol. 2015; 20(3): 337–344. doi: 10.3109/10837450.2013.867447. Epub 2013 Dec 18.

[32] Awasthi R., Rathbone M.J., Hansbro P.M., Bebawy M., & Dua K. Therapeutic prospects of microRNAs in cancer treatment through nanotechnology. Drug Deliv. Transl. Res., 2017; 8(1): 97-110. https://doi.org/10.1007/s13346-017-0440-1.

[33] Sharma P., Dando I., Strippoli R., Kumar S., Somoza A., Cordani M. & Tafani, M. Nanomaterials for Autophagy-Related miRNA-34a delivery in cancer treatment. Front. Pharma., 2020; 11: 1-16. doi: 10.3389/fphar.2020.01141.

[34] Gallardo M., Kemmerling U., Aguayo F., Tammy C., Bleak T.C., Juan P., Munoz J., & Calaf G.M. Curcumin rescues breast cells from epithelial mesenchymal transition and invasion induced by anti miR 34a. Int J. oncol., 2020; 56: 480-493. DOI: 10.3892/ijo.2019.4939.

[35] Zhu M., Zheng Z., Huang J., Ma X., Huang C., Wu R., Li X., Liang Z., Deng F., Wu J., Geng S., Xie C., & Zhong C. Modulation of miR-34a in curcumin-induced antiproliferation of prostate cancer cells. J Cell Biochem., 2019; 120:15616-15624. DOI: 10.1002/jcb.28828.

[36] Jahanbakhshi F., Dana P.M., Badehnoosh B., Yousefi B., Mansournia, M.A. Jahanshahi, M. Asemi, Z. and J. Halajzadeh, 2021. Curcumin anti-tumor effects on endometrial cancer with focus on its molecular targets. Cancer Cell Int., 21(120):1-7. https://doi.org/10.1186/s12935-021-01832-z.

[37] Geoffroy A., Saber-Cherif L., Pourié G., Helle D., Umoret R., Guéant J., Bossenmeyer-Pourié C., & Daval J. Developmental impairments in a rat model of methyl donor deficiency: effects of a late maternal supplementation with folic scid. Int. J. Mol. Sci. 2019; 20(973):1-14. doi:10.3390/ijms20040973.

[38] Nie D., Fu J., Chen H., Cheng J., & Fu, J. Roles of MicroRNA-34a in epithelial to mesenchymal transition, competing endogenous RNA sponging and its therapeutic potential. Int. J. Mol. Sci., 2019; 20(861): 1-14. doi:10.3390/ijms20040861.

[39] Li W., Wang Y., Liu R., Kasinski A.L., Shen H., Slack F.J., & Tang D.G. MicroRNA-34a: potent tumor suppressor, cancer stem cell inhibitor, and potential anticancer therapeutic. Front. Cell Dev., Biol. 2021; 9:1-21. doi: 10.3389/fcell.2021.640587

[40] Blandino G., & Di-Agostino S. New therapeutic strategies to treat human cancers expressing mutant P53 proteins. J. Exp. Clin. Cancer Res., 2018; 37 (1): 1-13. doi:10.1186/s13046-018-0705-7.

[41] Mendiratta G., Ke E., Aziz M., Liarakos D., Tong M., & Stites E.C. Cancer gene mutation frequencies for the U.S. Population. Nat. Commun. 2021; 12 (1):1-11. doi:10.1038/s41467-021-26213-y.

[42] Klco J.M., Mullighan C.G. advances in germline predisposition to acute leukaemias and myeloid neoplasms. Nat. Rev. Cancer., 2021; 21 (2): 122–137. doi:10.1038/s41568-020-00315-z.

[43] Zhou Y., Niu W., Luo Y., Li H., Xie Y., Wang H., Liu Y., Fan S., Li Z., Xiong W., Li , X., Ren C., Tan M., Li G., & Zhou M. p53/Lactate Dehydrogenase a axis negatively regulates aerobic glycolysis and tumor progression in breast cancer expressing wild-type P53. Cancer Sci., 2019; 110 (3), 939–949. doi:10.1111/cas.13928.

[44] Xiong J., Li G., Mei X., Ding J., Shen H., Zhu D., & Wang H. Co-Delivery of p53 restored and E7 targeted nucleic acids by poly (Beta-Amino Ester) complex nanoparticles for the treatment of HPV related cervical lesions. Front. Pharma., 2022;13: 1-12. doi: 10.3389/fphar.2022.826771.

[45] Zhou Y., Niu W., Luo Y., Li H., Xie Y., Wang H., et al. p53/Lactate Dehydrogenase A axis Negatively Regulates Aerobic Glycolysis and Tumor Progression in Breast Cancer Expressing Wild-type P53. Cancer Sci., 2019.110 (3), 939–949. doi:10.1111/cas.13928.